General Disclaimer

One or more of the Following Statements may affect this Document

- This document has been reproduced from the best copy furnished by the organizational source. It is being released in the interest of making available as much information as possible.

- This document may contain data, which exceeds the sheet parameters. It was furnished in this condition by the organizational source and is the best copy available.

- This document may contain tone-on-tone or color graphs, charts and/or pictures, which have been reproduced in black and white.

- This document is paginated as submitted by the original source.

- Portions of this document are not fully legible due to the historical nature of some of the material. However, it is the best reproduction available from the original submission.

NASA TECHNICAL MEMORANDUM

NASA TM X-62,377

NASA TM X-62,377

THE EFFECT OF HEAT TREATMENT AND TEST PARAMETERS ON THE AQUEOUS STRESS CORROSION CRACKING OF D6AC STEEL

William P. Gilbreath and Michael J. Adamson

Ames Research Center
Moffett Field, California 94035

September 1974

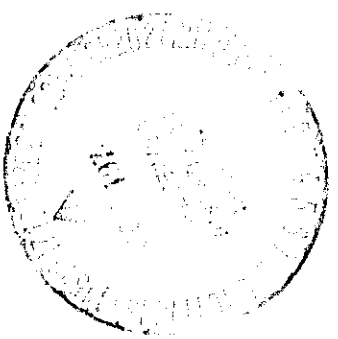

The Effect of Heat Treatment and Test Parameters on the Aqueous Stress Corrosion Cracking of D6AC Steel

William P. Gilbreath[1] and Michael J. Adamson[1]

ABSTRACT: The crack growth behavior of D6AC steel as a function of stress intensity, stress and corrosion history and test technique, under sustained load in natural seawater, 3.3 percent NaCl solution, distilled water, and high humidity air was investigated. Reported investigations of D6AC were considered in terms of the present study with emphasis on thermal treatment, specimen configuration, fracture toughness, crack-growth rates, initiation period, threshold, and the extension of corrosion fatigue data to sustained load conditions. Stress history effects were found to be most important in that they controlled incubation period, initial crack growth rates, and apparent threshold.

KEY WORDS: stress corrosion, D6AC steel, high strength steel, toughness, seawater, failure, test method

---

[1]Ames Research Center, NASA, Moffett Field, Calif. 94035.

Introduction

D6AC steel has been extensively utilized in the aerospace industry because of its high strength and good toughness coupled with its relatively low cost. Major components on the F111 aircraft and on the Titan IIIC missile have been fabricated from D6AC, and current plans call for use of the alloy for the solid rocket booster (SRB) cases to be used in the Space Shuttle program. In the Shuttle program, the plans are to recover the used cases from the ocean after launch and to return them to the launch site for cleaning, refurbishment, and reuse. This program calls for a 10-20 launch reuse capability for each of the cases. Because these applications require long term exposure to various aqueous environments, a number of investigations [1-6] have examined the stress-corrosion susceptibility of D6AC steel under aqueous conditions.

It has been generally recognized within the last few years that in order to adequately characterize the stress-corrosion susceptibility of a particular alloy, it is necessary to determine at least the subcritical crack-growth kinetics and the threshold stress-intensity for the initiation of subcritical growth (K_{Iscc}). Also important, although less often studied, is the incubation period before crack-growth commences. When possibilities of variable heat treatments might exist either in design selection or in service, the effect of this factor must be adequately simulated in susceptibility testing. To insure useful design data, the effects of various test parameters must also be defined; of particular concern and controversy are selection of a proper test method (no ASTM standard method yet exists for stress-corrosion testing) and proper simulation of the service environment.

The purposes of the present paper are threefold: (1) To present new data on the stress-corrosion susceptibility of D6AC steel in one heat-treated

condition in a variety of simulated (Shuttle) service environments; (2) to compare the stress-corrosion data of various investigators on D6AC to determine both the effects of heat-treatment and the effects of test procedure on the incubation characteristics, crack-growth kinetics, and threshold stress-intensity for crack initiation (K_{Iscc}); and (3) to discuss the implications of the experimental observations on previously proposed mechanisms of stress corrosion of high strength steels. Specific points to be discussed include: The relative effects of natural seawater, synthetic seawater, and distilled water on the crack-growth behavior; the effects of heat-treatment (and resulting toughness); and, the possible influence of stress-intensity and stress history on the incubation period for crack-growth.

Experimental

The D6AC steel used in this investigation was produced by Cameron (Heat #52663) and the analysis, supplied by the vendor was: 0.47C, 0.82Mn, 0.008P, 0.005S, 0.19Si, 1.14Cr, 0.60Ni, 1.01Mo, 0.10V and the balance Fe (all in weight percent).

Specimens were machined from the D6AC plate in two orientations so that the crack-growth direction was either transverse (T) or longitudinal (L) to the rolling direction.

Two different specimen types were used for the stress-corrosion experiments. One type was the compact tension (CT) specimen specified for fracture toughness testing (ASTM-399) and the other was a wedge-opening-loaded specimen having the dimensions of a CT specimen but loaded by an instrumented bolt in the manner suggested by Novak and Rolfe [7]. These two specimen configurations are shown in Fig. 1 and Fig. 2, respectively. In addition to being loaded by pins in a testing machine (the conventional procedure), a few (standard) CT specimens were loaded by a wedge which was forced into the

machined notch. This will be described more completely in a later section.

The CT specimen configuration provides valid plane strain fracture conditions and permits a straightforward determination of both stress intensity and crack length over a considerable range of crack length. For calibration purposes, a clip-on crack-opening gage was used to measure the mouth opening displacement, V, (between the knife edges of the specimen) for a known load, P, and a variety of crack lengths, a. The compliance values, C, defined as the ratio V/P, were empirically fit to a fourth degree exponential power function. The opening mode stress intensity factor, K, could then be determined from the relation [8]

$$K = \frac{V[E/2B(dC/da)]^{1/2}}{C}$$

where B is the specimen thickness and E is Young's modulus. Since the compliance, C, is a function of crack length (defined by the exponential power function), the above relationship can be used to determine K from a knowledge of any two of the parameters P, V, and a. (The same compliance relationship was used for the pin-loaded, wedge-loaded, and bolt-loaded specimens.)

Following machining, the specimens were commercially heat-treated to the following specifications [9]: The normalized material was vapor degreased, preheated in air to 800°K; austenitized (while protected by neutral salt) at 1175 ± 10°K (1625°F) for 6000 s; then quenched in rapidly agitated salt (60 to 1 volume ratio) to 495°K in less than 300 s and held for 1800 s. Following air cooling to 320°K, the specimens were stress relieved in agitated salt at 500°K for 3600 s, then washed in hot water to remove all salt residues before double tempering in air at 900°K, for periods of 7000 s each. Finally, the specimens were grit blasted, and, in some cases, polished

to make it easier to view the subsequent crack-growth. The temperature was monitored and controlled during the heat treatment by thermocouples placed in drilled holes in two of the specimens. Tensile specimens were simultaneously heat treated with the fracture specimens. Average mechanical properties produced by this heat treatment, as determined for three specimens, are listed in Table 1.

TABLE 1. Average Mechanical Properties of D6AC Plate

Yield Strength		Ultimate Strength		Elongation	Reduction in Area	Hardness
MNm^{-2}	KSI	MNm^{-2}	KSI	% in 2.5 cm	%	R_c
1440	209	1520	220	15	43	45

Following isopropanol and distilled water washing, the specimens were fatigued to produce a starter crack. They were cycled in a tension-tension mode for about 100,000 cycles to form a flaw from 4 to 10 mm in length. During fatiguing, the specimens were loaded to impose a maximum calculated stress intensity at the crack tip of roughly 45 $MNm^{-2}m^{1/2}$ (40 KSI $In^{1/2}$).* The initial crack length (a_o) was visually determined on both faces as the distance from the load line center to the fatigue crack tip. The specimens were then stored in a desiccator until used.

As stated earlier, the two primary indicators of a material's susceptibility to stress-corrosion cracking are the rate of environment-induced, subcritical crack-growth and the threshold stress-intensity value, K_{Iscc}. The test method employed to obtain information on these two factors was to load the precracked specimens to some calculated initial

*In a few tests, somewhat different stress-intensities were used for fatiguing. The effects of these tests will be discussed in conjunction with Table 3.

stress-intensity level, and to maintain the crack mouth opening displacement constant thereafter. If crack extension then occurred due to stress-corrosion cracking, the load would decrease and cause a corresponding decrease in K. By measuring the rate of change in compliance at various K levels, it was possible to calculate crack-growth rates as a function of K. Under these test conditions, the crack would be self arresting as K decreased below the threshold value, so that K_{Iscc} could be determined from the same test. The value of the initial stress intensity, K_{Io}, for these tests was selected to be less than the fracture toughness, K_c, but usually greater than the stress-intensity used for fatigue pre-cracking, K_{If}. Methods of measuring compliance (and compliance changes) involved measuring both V and either instantaneous load, P, or crack length, a. While crack-growth could be detected from either load changes or observations of crack length changes, the changes in load were the more sensitive indicator. Therefore, it was much easier to detect crack initiation in those specimens loaded in a testing machine or with an instrumented bolt (for which load changes could be monitored) than it was for specimens loaded by a wedge. These latter specimens had the advantage of simplicity, however, in that their use did not tie up either a testing machine or other instrumentation for the relatively long test period required for these experiments. The instrumented bolts were designed for this program and represented a good compromise between the use of pin-loading in a test machine and simple wedge-loading. These bolts were easily calibrated to give reliable load values and provided essentially the same information (albeit with somewhat less accuracy) as did the load cell of the testing machine.

Tests were conducted in four different aqueous environments: Distilled water, 3.3 percent sodium chloride solution, filtered Pacific seawater

(1.023 s.g.) and moist air (principally at 90 percent r.h.). In the first three cases, both static and circulating environments were used. For those specimens under load in the test machine, the water was continuously circulated around the notched region of the specimen. This was accomplished by attaching a cylindrical plastic envelope to each face of the specimen (with silicone rubber adhesive), covering the expected crack extension area as well as the notch-tip region. The tail of the notch was filled with more adhesive to form a complete channel across the notch mouth such that the fluid could circulate through the notch tip and exit by crossing the other face. In this manner, the test machine, clip gage, and grips were protected from corrosion and any possible galvanic effects. Flow quantities were around five cm^3 of aqueous solution per minute and the reservoir was renewed periodically.

For tests under static conditions with wedge- and bolt-loaded specimens, the specimens were simply immersed in the solution to above the notch-tip. For the bolt-loaded specimens, care was taken to avoid contact between the bolt and the water. For the wedge-loaded specimens, the wedge was made from identically heat-treated D6AC. The solutions used for the static tests were usually renewed daily. Bolt- and wedge-loaded specimens were employed in the high humidity experiments. These tests were conducted in a closed plastic case, which contained temperature and humidity sensors and a fan for circulating moist air from a reservoir over the specimens. Crack growth in the wedge-loaded specimens was monitored by a cathetometer and in the bolt-loaded specimens by recording the strain output (load decrease).

RESULTS

Fracture Toughness Evaluation

Fracture toughness determinations were made on several CT specimens

using the prescribed American Society for Testing and Materials (ASTM) method [10]. Two types of load-displacement curves were observed in these tests. Most specimens exhibited elastic behavior terminating with an abrupt break, signaling pop-in. These specimens yielded fairly reproducible fracture toughness values on all specimens tested after fatigue cracking, but prior to stress-corrosion cracking. Other specimens were toughness tested subsequent to stress-corrosion cracking, both prior to and after natural crack arrest. With these specimens, both linear and curvilinear load-displacement curves were observed. When pop-in occurred (linear curves), uniformly high values of K_{Ic} were obtained (Table 2) as was the case with those specimens tested prior to aqueous exposure. When pop-in did not occur and the load-displacement relation became curvilinear, a 5 percent secant to the linear portion intercepted the curve to give K_Q (non-valid K_{Ic}) values as low as 84 $MNm^{-2}m^{1/2}$. The nature of the curve, particularly the deviation from linearity, is indicative of a non-valid test [10].

TABLE 2. Fracture Toughness of D6AC Steel

Specimen	Crack Length (cm)	Roll Direction	Fracture Toughness $MNm^{-2}m^{1/2}$	Fracture Toughness KSI $In^{1/2}$
1	1.57	T	124	113
2	1.63	L	121	110
3	2.77	T	117	106
4	3.91	L	119	108
5[a]	4.45	T	84	76
6[a]	4.24	L	91	83

[a]Non-valid test

Stress Corrosion

The data for crack-growth as a function of stress intensity for the four environments—natural seawater, 3.3 percent NaCl solution, high humidity and distilled water—are shown in Fig. 3. Because of the expected long-time exposure of the SRB material to natural seawater, most exposures were performed in this medium and results from the other environments are related to these. Other results are described which relate to the effect of changing environments, incubation time, and load history.

The crack growth rate versus stress intensity results are characterized by three distinct growth rate regions. Below a stress intensity of about 20 $MNm^{-2}m^{1/2}$, crack-growth did not take place. As the stress intensity on specimens in natural seawater, synthetic seawater (i.e., 3.3 percent NaCl), and distilled water decreased to this value, the growth rate became immeasurably small (less than 10^{-10} m s^{-1} or 10 μinch hr^{-1}). For stress intensities above this (apparent) threshold up to 100 $MNm^{-2}m^{1/2}$, the growth rate was relatively insensitive to changes in stress intensity. In this region, the growth rates in both natural seawater and the 3.3 percent salt solution were equivalent and increased from about 5 to $20x10^{-9}$ m s^{-1} with increasing K. Although the data show considerable variance, the rates in distilled water appear to fall in the lower part of the scatter band. A least squares analysis of the data, up to stress intensities of 80 $MNm^{-2}m^{1/2}$, showed the pure water rates to be about 60 percent of the saline data. Additionally, an increase in rate was found in the case of several specimens in which seawater was substituted for distilled water after crack-growth initiation. Above 100 $MNm^{-2}m^{1/2}$ (as K_{Ic} was approached), the crack-growth rates in the three liquid environments became quite dependent on stress intensity and rapidly accelerated. In distilled water, the rate in this

region appeared indistinguishable from the rates exhibited in the seawater solutions.

Figure 3 also shows data indicating that slow crack-growth occurred under high humidity conditions (95 ± 3 percent r.h.) at stress intensities in the region of 50 $MNm^{-2}m^{1/2}$. It was found from a number of specimens subjected to stress intensities between 50 and 100 $MNm^{-2}m^{1/2}$, that crack-growth could not be directly initiated in this environment. But, for the one specimen shown, growth was initiated in distilled water and found to continue when the specimen was placed in high humidity conditions. The rate shown is the steady state value achieved after 15 days. Reducing the humidity to 40 percent arrested the growth.

No differences in crack-growth rate were discernible, beyond experimental scatter, between the CT specimens that were wedge-loaded or pin-loaded and the bolt-loaded WOL specimens. Similarly, no effect of roll direction on the crack-growth rates was observed.

Table 3 shows the elapsed time between loading in the environment and the first indication of crack-growth as a function of imposed stress intensity for the specimens examined. Also tabulated are three other parameters: (1) The stress intensity ratio, defined as the imposed stress intensity divided by the maximum stress intensity during fatigue precracking (K_{Io}/K_{If}); (2) the particular aqueous environment, and (3) the loading method used. Several observations may be made from these data concerning the incubation period. These observations will be enumerated and discussed in a later section.

It was usually observed that the initial (following incubation) crack-growth rate was different from the rate observed at a given stress intensity after several days of crack-growth. The initial rate, which could either

TABLE 3. Crack Growth Initiation Periods in D6AC Steel

Initial Stress Intensity K_{Io} $MNm^{-2}m^{1/2}$	K_{Io}/K_{If}	Environment	Loading Mode	Incubation Period Hours
120	2.5	Seawater	Wedge	1
112	2.4	Distilled water	Wedge	20
112	2.4	Seawater	Bolt	0.2
110	1.8	3.3% NaCl	Wedge	13
104	2.4	3.3% NaCl	Wedge	5
98	2.2	90% R.H.	Bolt	> 600
88	1.9	Seawater	Testing machine	0.5
85	2.0	75% R.H.	Wedge	> 350
82	1.8	Distilled water	Testing machine	1
73	1.04	Distilled water	Testing machine	120
71	1.6	95% R.H.	Bolt	> 200
69	1.5	Distilled water	Wedge	180
66	1.26	Distilled water	Testing machine	1
62	1.36	Seawater	Bolt	5
55	0.92	Distilled water	Wedge	> 340
52	1.22	90% R.H.	Bolt	> 800
48	0.95	Seawater	Bolt	> 500
47	1.18	Seawater	Wedge	210
47	1.16	Seawater	Testing machine	4
41	0.93	Seawater	Testing machine	> 105
38	1.20	Seawater	Bolt	13

be a good deal faster or slower than the steady-state rate, depended on the load history. This behavior is illustrated in Fig. 4. Curve 1 is typical of a specimen either loaded in the environment or placed in the environment immediately after loading. Following the incubation period, the crack-growth rate would accelerate over a several day period until a steady-state rate was achieved. Conversely, when the stress intensity was increased (curve 2) on a specimen which was either cracking or was held for a period at a lower stress intensity, the initial rate was greater than the steady-state rate. For specimens with propagating cracks, a sudden decrease in stress intensity (curve 3) would arrest the growth until a new incubation period had elapsed and a new steady-state rate was achieved.

Discussion

The results of these tests on D6AC steel, heat-treated in the manner described, are in essential agreement with the results of previous investigations [1-6] performed on material heat-treated to different specifications. The heat-treatment used here omits the usual "Aus-Bay" quench (which would follow austenitizing) and provides for a rapid quench to avoid bainite formation. Thermocouple records showed that the high volume-ratio, rapidly agitated salt bath reduced the temperature at center thickness of the specimen from 1180°K to below 550°K in 140 s. This rate undoubtedly approaches the rate achieved in the oil quenches that normally produce equally high toughness, but which, without the accompanying "Aus-Bay" quench, causes dimensional instability.*

In Table 4, several results from this study are compared with previous

*No warpage or dimensional changes were observed in either the 2.5 cm thick fracture specimens or 0.625 cm thick tensile specimens heat-treated in the present study.

results. It can be readily seen that while the quench rate causes only minor changes in material strength level, it can cause significant differences in fracture toughness. The toughness values range from a low of 50 $MNm^{-2}m^{1/2}$ for 4 cm thick material quenched at a slow rate to a high of 120 $MNm^{-2}m^{1/2}$ measured in this study. (Note: The value of 125 $MNm^{-2}m^{1/2}$ reported by Pionke [5] was measured with a non-standard surface-flawed specimen and must therefore be considered questionable.) The toughness values measured in this study were found not to be dependent on orientation, with both longitudinal and transverse specimens giving identical values.

Although the fracture toughness values were found to be quite sensitive to heat treatment, the values of the threshold stress intensity for stress-corrosion cracking, K_{Iscc}, were essentially independent of heat treatment. With only one exception, all investigators measured a K_{Iscc} value of about 20 $MNm^{-2}m^{1/2}$ for both distilled water and seawater environments. (The one anomalous value of 10 $MNm^{-2}m^{1/2}$ was obtained by Hagemeyer and Hillhouse [3] on material having an undefined heat treatment.) This same K_{Iscc} value was measured using several specimen types, including surface flawed, compact tension, wedge-opening-loaded, and contoured double coutilever beam; additionally, it was measured in the present study using pin-loading, bolt-loading, and wedge-loading. This good agreement gives assurance that several test methods should be useful for developing K_{Iscc} data.

Figure 5 compares crack-growth rate data determined in the various investigations [1-6] with the data of this study. The scatter bands shown on the curves representing the data of this investigation and the data of Feddersen, et al [4], represent the maximum scatter observed in a fairly large number of tests. This scatter contains the effects of different specimen types, different environments (distilled, seawater), different

loading methods, etc. The two data points representing the crack-growth rate data of Amateau and Kendall [6] were derived from corrosion-fatigue results. By comparing the sustained-load and corrosion fatigue results of both Masters and White [1] and Feddersen, et al [4], at equivalent environmental conditions, stress ratios, and cyclic frequencies, it was possible to estimate a proportionality factor between corrosion-fatigue growth rates and sustained-load growth rates. This factor was used to calculate the two (equivalent) sustained-load data points shown for Amateau and Kendall. As can be seen in Fig. 5, the kinetic data from all the investigations are in good correspondence considering the large number of material and test variables included. The agreement is especially good at low stress intensities ($< 50\ MN^{-2}m^{1/2}$) where the average rates vary from one another by less than a factor of 3. At higher stress intensities, all data except those of Feddersen, et al, are still in good agreement, and the curves have the shape generally expected for environment-induced crack-growth [11]. The reason for the divergence of the data of Feddersen, et al, at the higher stress-intensities cannot be explained at this time; however, it should be noted that these authors report crack-growth rate data for stress intensities which are greater than the reported fracture toughness values. In both the present investigation and in the study by Feddersen, et al, it was noted that the average crack-growth rates in distilled water were slightly less than those in seawater. However, the differences in rate were less than the scatter of the results for crack-growth in seawater alone. This observation along with the observation that there were no detectable differences in either K_{Iscc} values or growth rates in synthetic seawater (3.5 percent NaCl) as opposed to natural seawater suggests that precise simulation of the environment is not necessary in determining the sensitivity of D6AC to aqueous stress-corrosion cracking.

The few tests that were conducted on D6AC in humid air appear to indicate that stress-corrosion cracks cannot be initiated in this environment but that, once initiated elsewhere, crack-growth can be supported in high humidity environments. While no previous studies have directly examined this point, there is evidence from corrosion fatigue work that humid air will assist subcritical cracking. Several studies [1, 5, 6] have demonstrated that fatigue crack-growth rates are greater in humid air than in dry air. The point might be raised as to why the crack-growth rates are not more nearly equal to the measured rates in water since previous studies [12] have shown that a continuous water film should form on surfaces near the crack tip at humidity levels considerably less than 95 percent R.H. It is possible that the anomalously low growth rates in humid air are caused by the continuous repassivation of the D6AC surface due, perhaps, to a high oxygen concentration in the water film. In any event, the data regarding slow crack-growth rates in humid air should be used with caution; a more conservative approach might be to assume that under some undefined service conditions, crack-growth in humid air might be expected to occur at rates equal to the rates measured in these studies for water.

The results shown in Table 3 indicate that an incubation period exists for the initiation of cracking of D6AC in aqueous environments. This observation has also been made by previous investigators [1, 3, 4] who have attempted to relate the length of this period to initial stress intensity, K_{Io}. The data of Table 3 show several interesting effects related to incubation. First, it is clear that the *apparent* incubation period is strongly dependent on the method of measuring crack-growth. Visual inspection methods of the type employed for wedge-loaded specimens led to estimated times which were as much as 100 times longer than did instrumented methods based on measuring compliance changes (machine-loading and bolt-loading).

Presumably, more sensitive instrumented methods such as acoustic emission would yield still shorter apparent incubation periods. This is suggested by the results of ref. [3] which indicated incubation times which were 50-100 times shorter than those measured in this study and which used acoustic emission as the detection method. Second, the results show no effect of the type of environment (i.e., distilled water versus seawater) on the length of the incubation period. This is consistent with previous observations [4]. Finally, and most importantly, the length of the incubation period appears to depend strongly on the specimen stress-history -- namely, the ratio of the initial sustained stress intensity, K_{Io}, to the maximum fatigue stress intensity, K_{If}. Actually, as can be seen from Fig. 6, this parameter (K_{Io}/K_{If}) provides a much better correlation with incubation time than does K_{Io}, raising some question as to whether incubation time is actually a function of K_{Io} as suggested by previous workers [13]. Although it might be argued from the data of Table 3 and Fig. 6 that there is a general trend toward longer incubation periods at lower stress intensities, two factors other than stress intensity probably play an important role in this lengthening. First, there is generally a decrease in stress-ratio as stress intensity is decreased, thus leading to longer times. (For those cases where there is not a corresponding decrease in stress ratio, no trend is apparent.) Second, it is easier to detect crack-growth at high rather than at low stress intensities because of the faster crack-growth rates at high stress intensities. The entire question of incubation periods undoubtedly deserves further study before it can be completely resolved. The observations of the effects of stress history are particularly important to clarify, as proper understanding may lead to pre-stress treatments which might result in improved stress corrosion resistance of particular D6AC components (including Shuttle SRB cases).

Figure 4 shows the effect of stress history on the initial (non-steady) rate of crack propagation. This result appears quite similar to the effect that the stress intensity ratio was shown to have on the incubation period and probably stems from an identical cause. Harrigan, et al [2], although not reporting on crack initiation directly following precracking, have considered the effect that decreasing the stress intensity has on a propagating crack in D6AC. In all cases, a new incubation time, strongly dependent on the magnitude of decrease, is required. They further noted [2] "a short transient between no growth behavior and the steady growth behavior". In an earlier paper [13] by two of these authors, it is pointed out that a zero incubation time occurs when stress intensity is increased in the case of AISI 4340 steel. No mention is made in either paper of the initial rates observed when the stress intensity on a propagating crack is increased.

The results presented here and in earlier evidence [2, 13, 14] suggest that two mechanisms play a role in determining crack-growth rates in D6AC. Harrigan, Dull and Raymond [2] for D6AC and AISI 4340, and Dull and Raymond [13], for AISI 4340, explain the observed incubation periods following reduction of stress intensity in the case of D6AC and following precracking, in 4340 on the basis of a hydrogen charging mechanism. By this mechanism, the product of stress state and chemical potential must reach a certain value before cracking can commence; thus, reduction of stress intensity on a propagating crack would necessitate a delay period in order for the hydrogen charge at the crack tip to increase to a value sufficient to restore the stress-potential product. These investigations failed to report on the transient growth behavior preceding steady-state conditions which could have provided important collaborative evidence.

The present work shows the existence of such transients (Fig. 4) which

are lower than steady state under initiation conditions (including decreases in stress intensities with propagating cracks) and are greater than steady state when the stress intensity on such cracks is increased. These results indicate that the hydrogen charge accumulated before the stress intensity was changed may be dictating the initial rates at the new stress intensity level. But, in addition to this chemical effect, the present work shows (Table 3) that there must also be a mechanical effect since fatigue precracking of D6AC at stress intensities near those imposed during environmental loading can drastically increase incubation periods. Carter [14] reports similar results for AISI 4340 (prestressing doubled K_{Iscc}) and suggests that load reduction subjects the crack tip to compressive forces from the surrounding elastically strained material. Such compression would lessen the effective imposed stress intensity and the magnitude of the effect would be dependent on the strain-hardening characteristics at the crack tip. Such a mechanism would not only affect the threshold, as Carter shows [14], but would also affect the transient behavior seen on decreasing the stress intensity imposed on a propagating crack in D6AC since this material exhibits (as opposed to AISI 4340 [14]) a stress intensity dependent crack-growth velocity (Fig. 3). It thus appears that both stress history and corrosion history influence crack-growth velocities in D6AC.

CONCLUSIONS

(1) D6AC steel in a high toughness condition exhibits substantially similar stress corrosion behavior in natural seawater, 3.3 percent NaCl solution, and distilled water: A threshold at 20 $MNm^{-2}m^{1/2}$, a slow crack-growth (10^{-8} m s^{-1}) at moderate stress intensities, and sharply increasing rates as K_{Ic} (120 $MNm^{-2}m^{1/2}$) is approached.

(2) The thermal treatment employed in the investigation produces the highest

reported toughness for D6AC. Collation with results of earlier workers showed that differences in heat treatment, roll direction, environment, and sample configuration have very little effect on threshold, flaw growth kinetics or the intrinsic incubation period for crack initiation.

(3) In D6AC, stress history and corrosion history are basic to certain aspects of its stress-corrosion behavior. Incubation, while weakly dependent on imposed stress intensity, is closely related to prestressing or fatigue precracking effects. Transient growth, before steady-state rates are attained, is inferred to depend on accumulated hydrogen potential as well as stress effects.

(4) Additionally, other implications may be drawn that concern Shuttle SRB application of D6AC. The fracture toughness of the material (which must be in accord with expected operating stresses) is nearly wholly dependent on the quench used in the thermal treatment. Crack-growth rates and threshold of the selected material will be virtually independent of the heat treatment, test technique, specimen configuration and aqueous environment constituents. This factor should considerably reduce the complexity of simulation necessary for viable design evaluation. Although the extremely low threshold indicates that environment assisted subcritical flaw extension can occur at much less than planned operating stress, the very slow growth requires considerable (ten day) ocean exposure before flaws reach critical size for fracture under proof test. Proof testing should not only detect such critical size flaws but would also tend to blunt subcritical flaws and greatly increase the environmental incubation period for their growth initiation.

References

[1] Masters, J. N. and White, J. L., Technical Report AFML-TR-70-310, The Boeing Company, Seattle, Washington, 1971.

[2] Harrigan, W. C., Dull, D. L., and Raymond, L., ASTM Special Technical Publication 536, American Society for Testing and Materials, Philadelphia, PA, 1972, pp. 171-181.

[3] Hagemeyer, J. W., and Hillhouse, L., Research Report ERR-FW-1114, General Dynamics, Fort Worth, Texas, Dec. 1970.

[4] Feddersen, C. E., Moon, D. P., and Hyler, W. S., MCIC-72-04, NTIS, U. S. Dept. of Commerce, Jan. 1972.

[5] Pionke, L. J., and Garland, K. C., Contractor Report CR 120160, NASA, Dec. 1973.

[6] Amateau, M. F., and Kendall, E. G., Air Force Report No. SAMSO-TR-71-186, The Aerospace Corporation, Los Angeles, CA., Sept. 1971.

[7] Novak, S. R., and Rolfe, S. T., Technical Report No. 89,018-026(1), United States Steel, Monroeville, PA., May 1968.

[8] Gilbreath, W. P., and Adamson, M. J., Technical Note TN D-7604, NASA, Feb. 1974.

[9] Jacobs, Samuel, United Technology Corporation, Sunnyvale, CA., private communication.

[10] Brown, W. F., Ed., ASTM Standard Technical Publication 463, American Society for Testing and Materials, Philadelphia, PA., 1970, pp. 249-269.

[11] Williams, D. P., *Int. J. Fract.*, 1973, Vol. 9, pp. 63-74.

[12] Johnson, H. H., and Williams, A. M., *App. Mat. Res.*, 1965, pp. 34-40.

[13] Dull, D. L., and Raymond, L., *Met. Trans.*, 1972, Vol. 3, pp. 2943-2947.

[14] Carter, C. S., *Met. Trans.*, 1972, Vol. 3, pp. 586-587.

TABLE 4. Reported Properties of D6AC Steel

Ref.	Specimen Type[a] Thickness (cm)	HEAT TREATMENT: Austinitize °K	Aus-Bay °K	Quench[b] K°	Snap Temper °K	Double Temper °K	Hrs	F_{ys} MNm^{-2}	F_{ys} KSI	K_{Ic} $MNm^{-2}\sqrt{m}$	K_{Ic} $KSI\sqrt{in}$	K_{Iscc}[c] $MNm^{-2}\sqrt{m}$	K_{Iscc}[c] $KSI\sqrt{in}$
Present Work	CT 2.5	1175		495 salt A	500	900	4	1440	209	120	109	20	18
	WOL 2.5	1175		495 salt A	500	900	4					20	18
1	CT .76	——not given——						1520	220	60	54		
	SF .76	——not given——						1520	220	88	80	17.6	16
2	CDCB 1.27	1190	800	495 salt C	375	1000	4	1550	225	65	59	< 22	< 20
3	WOL 1.7	——not given (Plate)——						1720	~250	111	101	10	9
	WOL 1.7	——not given (Forging)——						1720	~250	44	40	20	18
4	CT 2.0	1217	814	350 oil A		830	2	1455	211	105	96	20	18
	CT 4	1217	814	350 oil A		830	2	1455	211	99	90	20	18
	CT 2.0	1190	814	455 salt B		830	2	1500	218	88	80	20	18
	CT 4	1190	814	455 salt C		830	2	1500	218	50	45		
	CT 2.0	1190	814	495 salt B		830	2	1500	218	71	65		
	CT 4	1190	814	480 salt B		830	2	1460	212	66	60		
5	WOL .46	1175		495 salt B		872	4	1360	197	111	101	19.3	17.6
	WOL .46	1200	810	322 oil A		872	4	1345	195	114	104	18.8	17.1
	SF .91	——same——								125	114	< 22	< 20
6	CDCB .89	1217	800	350 oil A	480	828	2	1520	220	113	103	< 22	< 20
	CDCB .89	1189	800	495 salt C	480	828	2	1520	220	81	74	< 22	< 20
	CDCB .89	1189	800	480 salt B	480	828	2	1520	220	55	50	< 22	< 20

[a] Specimen configurations: CT, compact tension; SF, surface flawed; CDCB, contoured double cantilever beam; WOL, wedge opening loaded.

[b] Also indicates quench medium and relative circulation: A, high; B, medium; C, low.

[c] Threshold values are for an aqueous environment; both distilled or saline give similar results.

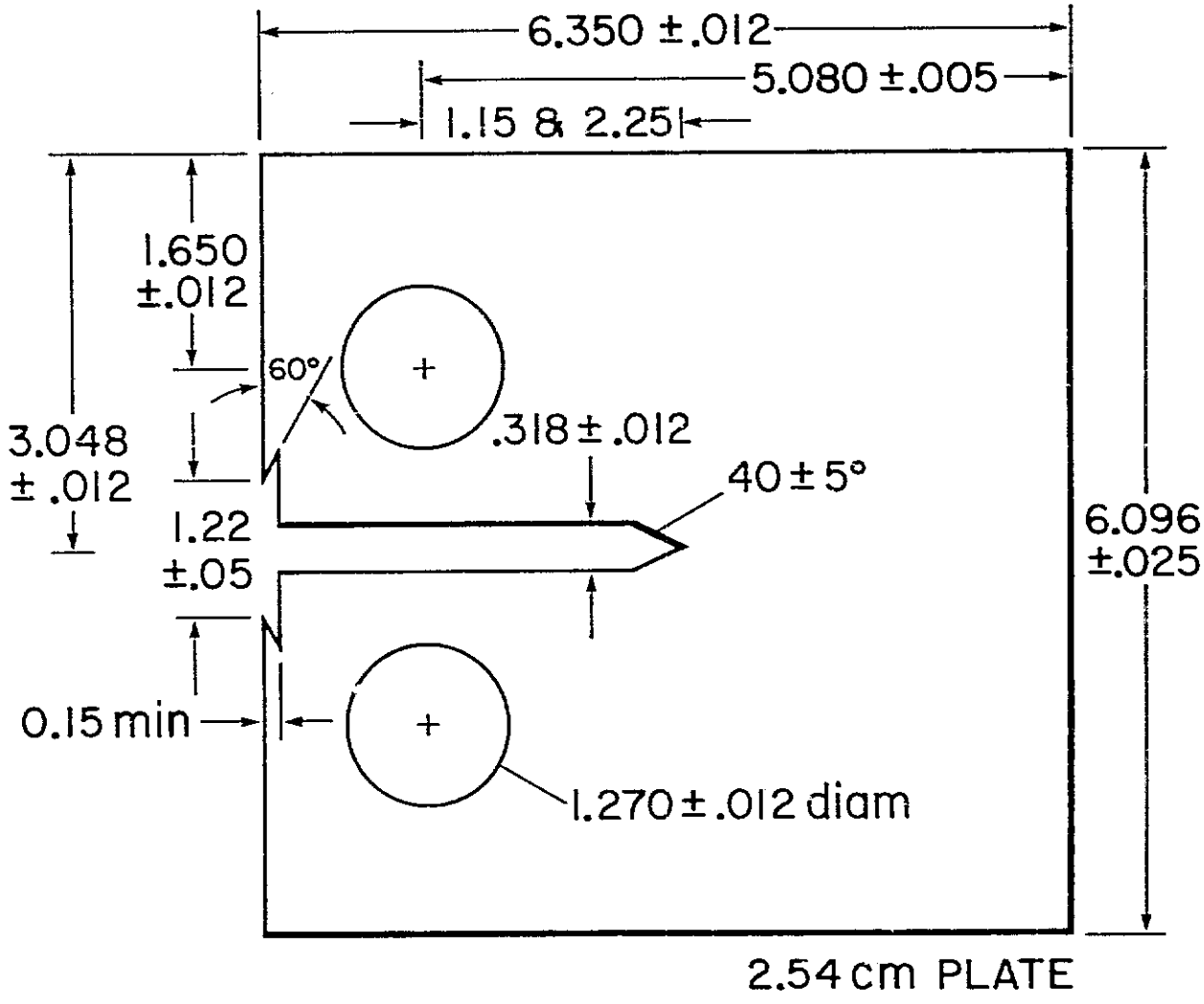

Fig. 1. Specimen configuration for stress corrosion cracking study. Dimensions in cm.

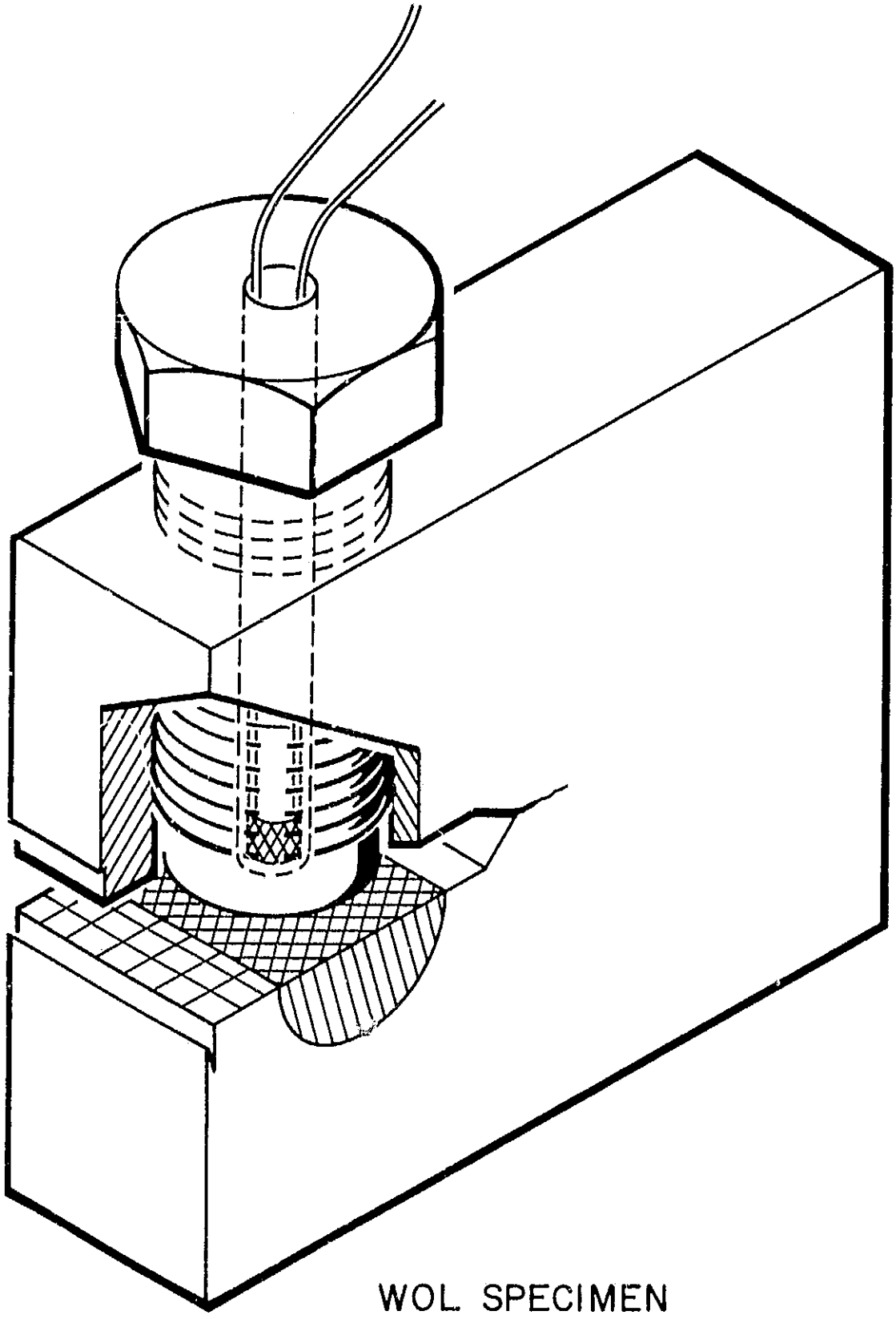

Fig. 2. Modified wedge opening loaded specimen with instrumented bolt.

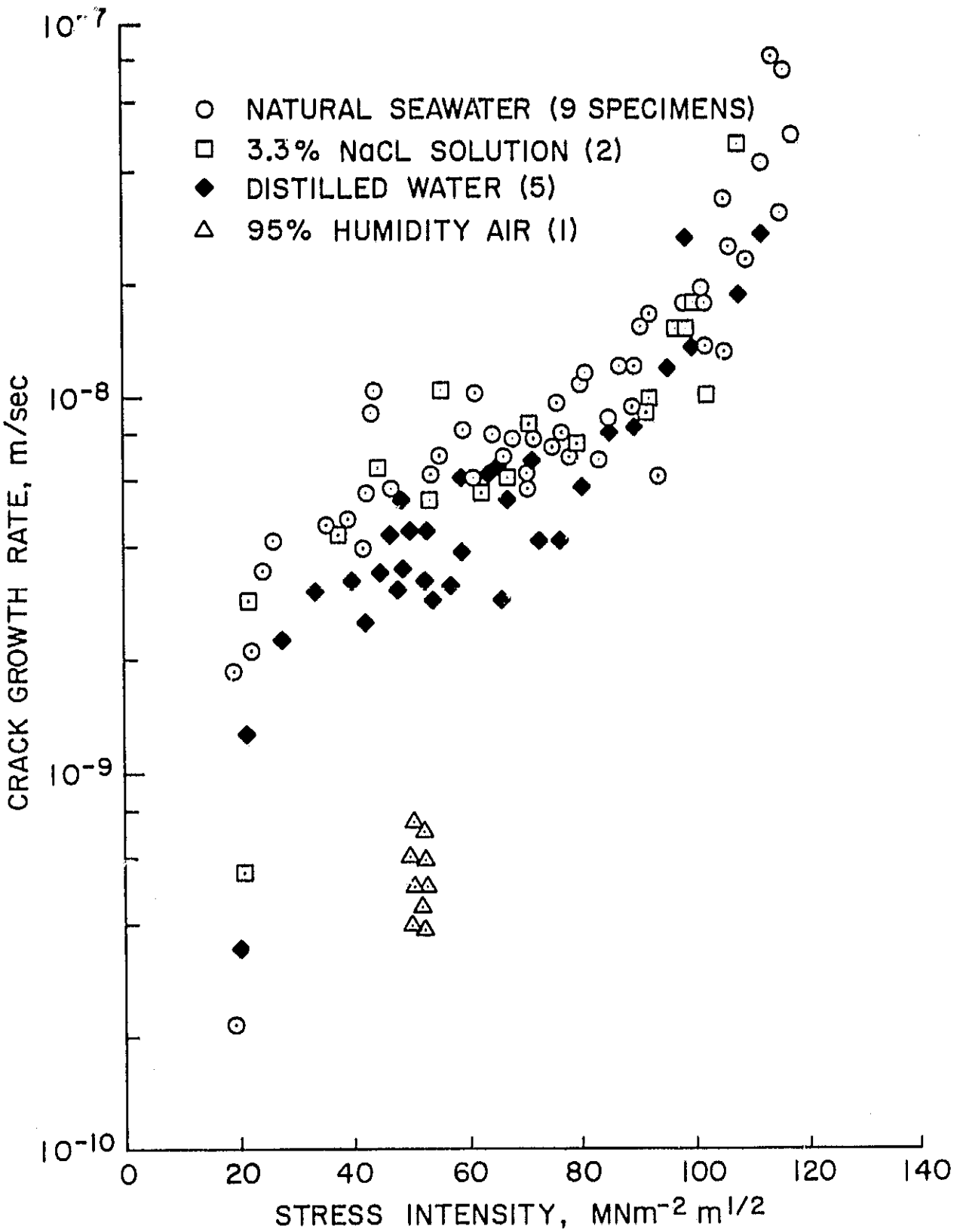

Fig. 3. Crack growth rates as a function of stress intensity for D6AC steel in aqueous environments.

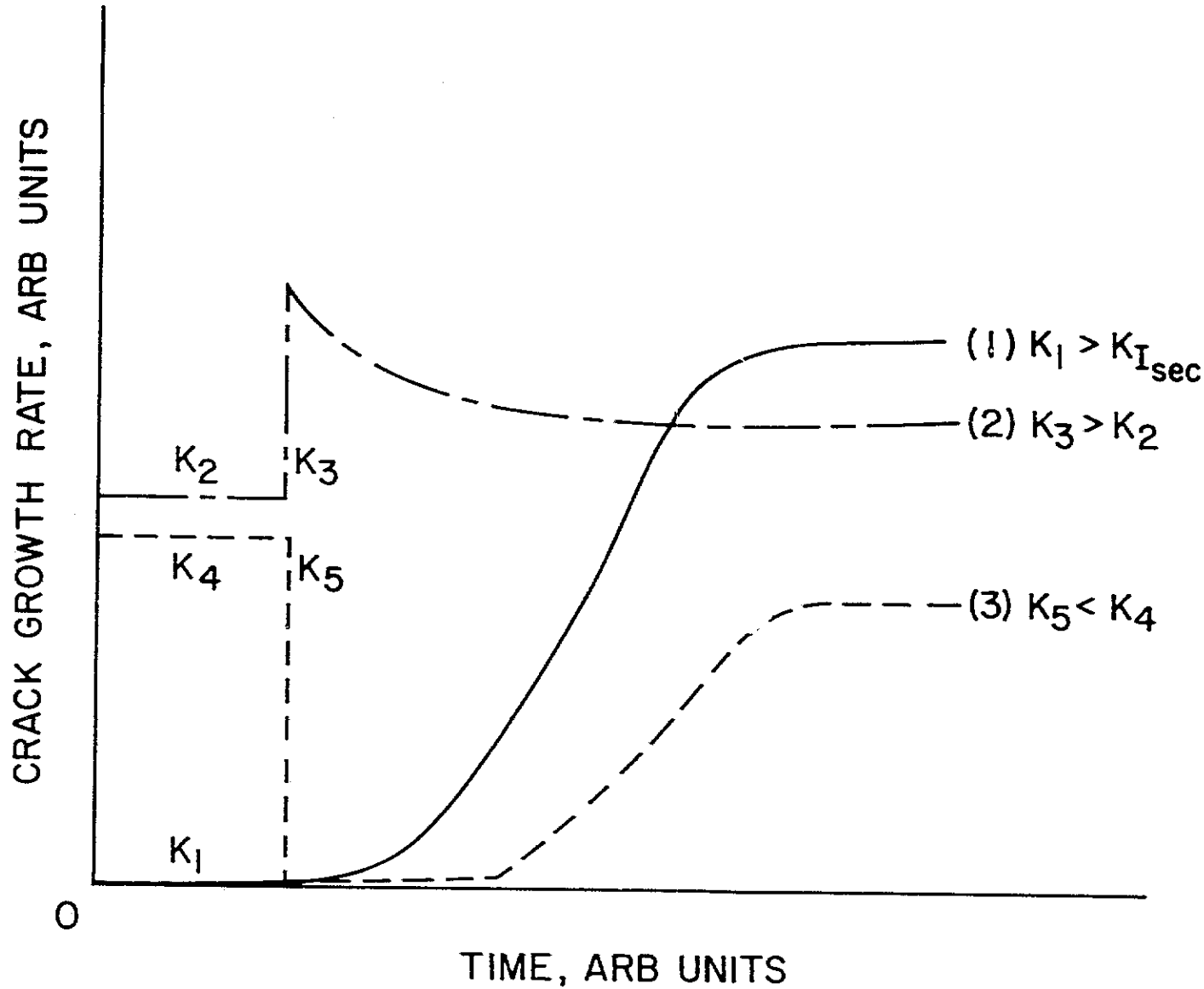

Fig. 4. Typical effect of load history on initial crack propagation rates in 6AC.

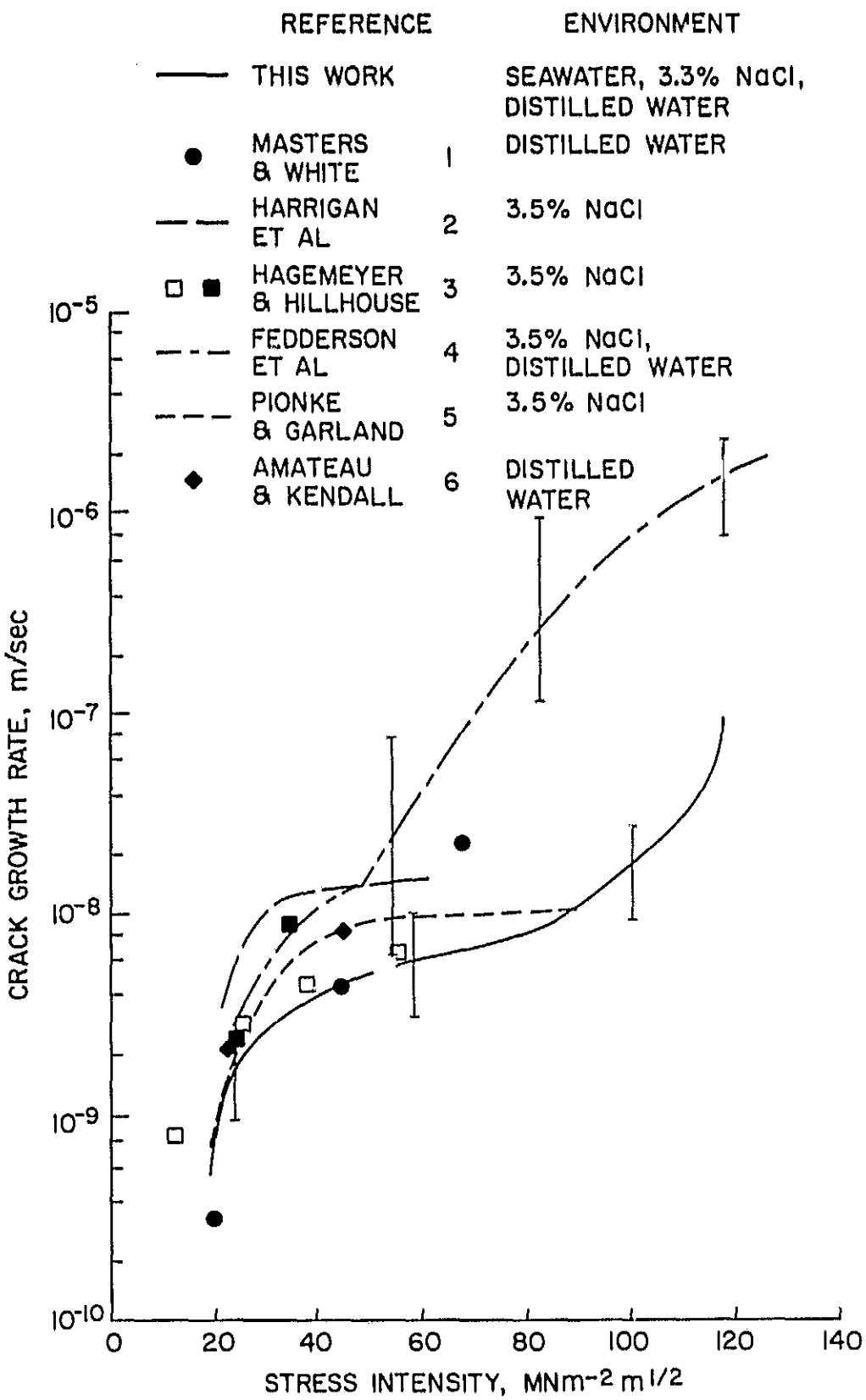

Fig. 5. Reported crack growth rates of D6AC steel as a function of stress intensity.

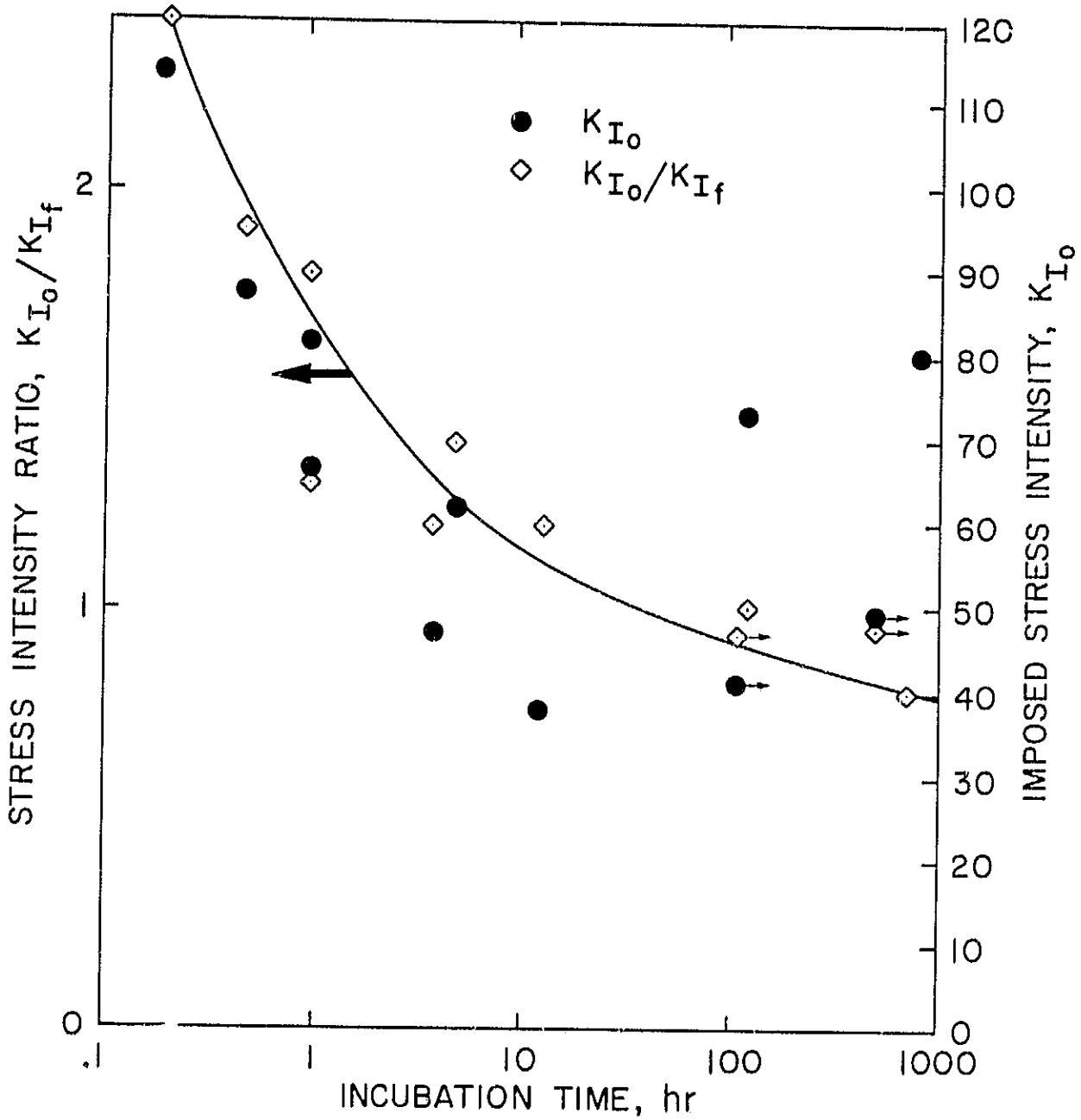

Fig. 6. Incubation periods for crack growth initiation of D6AC steel in aqueous environments as a function of stress intensity (K_{I_o}) and the ratio of stress intensity to fatigue stress intensity (K_{I_o}/K_{I_f}).